ORIGINAL RESEARCH

Frequency shifts and interaction strength of model hydrogen-bonded systems: new NBO and QTAIM characteristics

Boaz G. Oliveira

Abstract An innovative theoretical study of intermolecular properties of standard hydrogen-bonded complexes of $H_2O \cdots HCF_3$, $NH_3 \cdots HCF_3$, $H_2O \cdots HF$, and $NH_3 \cdots HF$ is presented in this work. Several computational strategies were used, so initially the MP2/6-311++G(d,p) level of theory was applied to determine the optimized geometries by which the structural parameters, electronic properties, and the stretch vibration modes of these systems were examined. By taking into account the infrared spectrum analysis, the frequency shifted either to the red- or blue-region is the principal interpretation upon formation of intermolecular complexes. Due to this, the analysis of the interaction strengths corroborates with these vibration behaviors, and besides, the Natural Bond Orbital calculations revealed systematic changes in the percentage of the s and p orbitals, by which the stretch deformations on the proton donors (HF and HCF_3) could be understood. In advance, it was quoted the appearing of intermolecular covalence in these complexes, and this event could be theoretically discovered through the topological computations based on the Bader's Quantum Theory of Atoms in Molecules.

B. G. Oliveira (✉)
Institute of Environmental Sciences and Sustainable Development (ICADS), Federal University of Bahia, Barreiras, BA 47801-100, Brazil
e-mail: boazgaldino@gmail.com

Introduction

Even after all these years, the hydrogen bond interactions are still considered one of the most studied themes in worldwide chemistry [1]. This prestige was acquired due the great importance and eminent influence of the H-bond attractions in the elucidation of several problems not only in chemistry [2, 3] but also in correlated areas, where among many of them we can cite the physics [4], spectroscopy [5], and biology [6] as the most privileged ones. Indifferently, it must be emphasized that the correct examination of the H-bond properties can be entirely compromised if the intermolecular basis of this interaction is not known in details [7]. In line with this, the routine adopted in hydrogen bond studies naturally leads to understanding of the interaction strength [8–11], where the proton acceptors containing lone electrons pairs (O, N, or S) often yield strong intermolecular contacts and many of them containing traits of covalence [12]. Is then, by this scenery that a lot of investigations have been performed always in seeking by the existence of covalence in hydrogen bonds [13].

In physics, a long time ago that intermolecular covalence has been researched [14], but on viewpoint of the theoretical chemistry this phenomenon was carefully taken into account only in recent years [12, 15]. In this context, here is presented a theoretical contribution based on the analysis of structural parameters, electronic properties, vibration stretch modes [16–23], and topological integrations [24] of intermolecular model systems formed by H_2O and NH_3 as acceptors of proton, while HCF_3 and HF represent the donating ones, namely as $H_2O \cdots HCF_3$, $NH_3 \cdots HCF_3$, $H_2O \cdots HF$, and $NH_3 \cdots HF$. These systems have already been analyzed in several circumstances [8, 12, 25, 26] either by theoretical or experimental procedures, but the main goal of

this work aims to demonstrate the relationship between the interaction strength determined via supermolecule approach and the charge density concentration, and at this current time the purpose is not simply the identification of the intermolecular covalent character but how this event influences in the appearing and displacement of the red- and blue-shifts in the proton donors [27].

The theoretical procedures to analyze hydrogen bond properties request a quite efficient computational method. It is usual to find in several works that MBPT (Many-Body Perturbation Theory) [28] at the MP2 second-order level [29] is the most recommended theoretical parameterization because the electronic correlation is completely taken into account. As direct consequence, the available experimental data derived from structure or vibration sources are precisely reproduced [30]. Also, the requirement of a complete basis set is required because beyond the description of heavy atoms (C, N, and O), an overcare with the overlap of the intermolecular wave function reflected in the Basis Sets Superposition Error (BSSE) is mandatory [31]. Due to this, the MP2/6-311++G(d,p) method was chosen as the level of theory to be used in this work, and it is expected that the structural, electronic, and vibrational properties of the $H_2O\cdots HCF_3$, $NH_3\cdots HCF_3$, $H_2O\cdots HF$, and $NH_3\cdots HF$ complexes can be successfully evaluated.

On the spectroscopy context, the stretch frequency modes of donors and acceptors of protons are the mainstream in any intermolecular study of hydrogen-bonded complexes [32]. It is well-known that variation on these modes often leads to the arising of the red- and blue-shift effects, which are displacements to the regions with lower and higher energies in the infrared spectrum [33]. In turn, these events are consequences of weakness or strengthening in the proton donor oscillator, and these occurrences can be suitably explained by means of the molecular orbital analysis, in particular ruled by the criteria of the Natural Bonding Orbital (NBO) [34]. Besides the contribution of the atomic orbitals (s or p) to the formation of the chemical bond as well as it should be highlighted that this is closely related with the variation in the stretch frequencies of the monomers upon the formation of the complex (A···B), the NBO calculations also can provides the interaction energy (ΔE) between pairs of atoms (A and B) into a chemical bond as follows [35]:

$$\Delta E_{n(A)\to\sigma*(B)} = q_{n(A)\sigma*(B)} \frac{\langle n(A)|F|\sigma*(B)\rangle^2}{\left[\varepsilon_{n(A)} - \varepsilon_{\sigma*(B)}\right]} \tag{1}$$

where A and B symbolize the sub-parts (Y and HX) of a hydrogen bond (Y···HX), wherein Y is a high charge center formed by lone electron pairs or π bonds while B is a proton donor. Nevertheless, A and B also can be interpreted as any other atom that forms the chemical

bonds of the supermolecule. Since, the first investigations signed by Bader and Popelier [36, 37] up to the published works in the most recent years have clearly shown that the application of the Quantum Theory of Atoms in Molecules (QTAIM) [38, 39] is decisive in the characterization of the hydrogen bonds and others similar intermolecular interactions. On the hydrogen bond viewpoint, it is by the location of the bond critical points (BCP) that the electronic density and its Laplacian are modeled. The Laplacian shape is the cornerstone to identify if depletion or electronic accumulation shall occur within the internuclear region: $\nabla^2\rho > 0$ (close-shell contacts) and $\nabla^2\rho < 0$ (shared interactions). The first designation presents a low electronic density (ρ) on the BCP, and thereby it is used to examine the hydrogen bonds. About the second one, it is through this criterion that all covalent bonds are identified because high electronic densities are accounted if $\nabla^2\rho < 0$. Either covalent ($-G/U <1$) or non-covalent ($-G/U >1$), it is through the contributions of the kinetic electronic density energy (G) and potential electronic density energy (U) that the real bonding strength between two atoms can be unveiled:

$$2G + U = \left(\frac{\hbar^2}{4m}\right)\nabla^2\rho \tag{2}$$

In fact, the intermolecular properties of the $H_2O\cdots HCF_3$, $NH_3\cdots HCF_3$, $H_2O\cdots HF$, and $NH_3\cdots HF$ complexes have been exhaustively studied with a lot of publications documented in the specialized literature [40–43]. On the other hand, actually the complexes formed by these molecules are being re-examined in this current work although at light of the most recent theoretical approaches and novel perspectives, e.g., the intermolecular covalence. Thus, it is expected a great contribution in this field, mainly by considering the insertion of the infrared vibration study as fundamental analysis in this regard.

Computational details

The optimized geometries of the $H_2O\cdots HCF_3$, $NH_3\cdots HCF_3$, $H_2O\cdots HF$, and $NH_3\cdots HF$ hydrogen-bonded complexes were obtained through the application of the MP2/6-311++G(d,p) level of theory wherein all calculations were executed by the GAUSSIAN 03 W quantum software [44]. The computations of the orbital analysis and QTAIM integrations were all developed in GAUSSIAN 03 W through the activation of the following standard keywords: "POP = (NBO)" and "AIM = CHARGES." Besides some additional QTAIM calculations were made by the QBAIM 11.12.19 and AIMStudio 11.12.19 subunits pertaining to the AIMAll 11.05.16 [45] quantum package.

Results and discussion

Structural and vibration shifts

The equilibrium geometries of the $H_2O{\cdots}HCF_3$ (**I**), $NH_3{\cdots}HCF_3$ (**II**), $H_2O{\cdots}HF$ (**III**), and $NH_3{\cdots}HF$ (**IV**) complexes located at a minimum of the potential energy surface with total absence of imaginary frequencies are portrayed in Fig. 1. On this illustration, the bond lengths obtained by MP2/6-311++G(d,p) are also drawn, while the values of the isolated monomers are gathered in Table 1. If the Lewis acid–base concept was taken into account, it is acceptable that (**IV**) is shorter bonded rather than (**III**). In this same theory, but regarding the acid interpretation, actually these last complexes are the shortest bound ones than (**I**) and (**II**) because the hydrofluoric acid is a median strength acid. Meanwhile, the H-Bond distance values of 2.1964 (**I**), 2.2880 (**II**), 1.7310 (**III**), and 1.7023 (**IV**) are very shorter than sum of the tabulated van der Waals radii for H, O, and N, whose results for O$\cdots$H are 2.72 or 2.61 Å, whereas 2.75 or 2.64 Å are values corresponding to N$\cdots$H attraction [46, 47]. In according with Klein [48], although this empirical ensemble states the H-bond formation, this scenery is not common once the overwhelming majority of the hydrogen-bonded complexes have not intermolecular distances quite short like these ones. Furthermore, it must be worthwhile to mention that **I**–**IV** are relatively strong bonded complexes, and this statement may lead directly the assessment of drastic deformations on the bond lengths of the proton donors. In Table 1, the values of 0.0150 Å (**III**) and 0.0313 Å (**IV**) indicate that H–F is the most varied bond rather than 0.0015 Å (H–O in **III**) and 0.0016 Å (H–N in **IV**), respectively. This situation accords perfectly with the chemical literature of the hydrogen bonds, although an opposite behavior is verified in the rest of the systems. Respectively in **I** and **II**, a reduction of −0.0020 Å followed by a very soft one of −0.00002 Å were computed in the HC bond lengths in HCF_3. Of course, bonded systems such as **I** and **II** formed by long intermolecular distances often yield slight variations on the structures of the supermolecules, just like is observed in π complexes of acetylene and cyclic hydrocarbons as proton acceptors [49–51].

In conformity with the structural results discussed above, it should be expected a satisfactory relationship with the profile of the vibrational modes, and through the analysis of the results organized in Table 2 this occurs indeed. The shorter bound complexes (**III** and **IV**) present the new vibrational modes higher whose respective values are 223.2 and 265.7 cm^{-1}, where this last one is in good concordance with other theoretical results at CCSD(T) level of theory divulged by Botschwina and
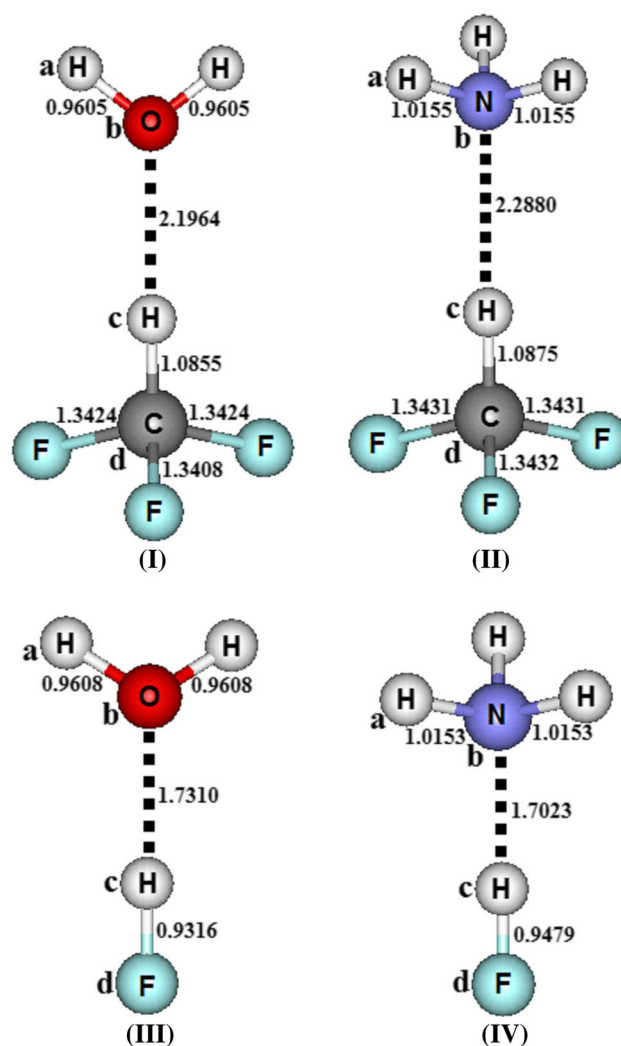

Fig. 1 Optimized geometries of the $H_2O{\cdots}HCF_3$ (**I**), $NH_3{\cdots}HCF_3$ (**II**), $H_2O{\cdots}HF$ (**III**), and $NH_3{\cdots}HF$ (**IV**) complexes obtained through the MP2/6-311+G(d,p) calculations

Oswald [52]. Moreover, it can be also highlighted that the absorption intensity values of 5.84 and 7.67 km mol^{-1} evince how much **III** and **IV** are intermolecular complexes strongly bonded. Only for comparison, the absorption intensity results for **I** and **II** are 0.54 and 0.73 km mol^{-1}, respectively. Regarding the proton donors, HCF_3 and HF, a direct relationship between the variation on their bond lengths and frequency shifts was found, in which both the red-shifts and blue-shifts are inserted. In **III** and **IV**, a natural increasing in r_{H-F} corroborate fully with the respective red-shift values of −347.2 and −718.3 cm^{-1}. In **I**, a reduction in r_{H-C} of HCF_3 associated with the blue-shift of +35.4 cm^{-1} is evidenced, but otherwise the less evident variation of −0.00002 Å in **II** manifests itself uncorrelated with a slight red-shift of −3.3 cm^{-1}, wherein a blue-shift even though sensitively displaced was expected, by the same insight pointed out by van der Veken and

Table 1 Values of the bond lengths on the monomers (H_2O, NH_3, HCF_3, and HF) as well as the variations on the complexes (**I–IV**) computed by the MP2/6-311++G(d,p) level of theory

Systems	Bonds		
	H–O	H–N	H–X
H_2O	0.9593	–	–
NH_3	–	1.0137	–
HCF_3	–	–	1.0872
HF	–	–	0.9166
I[a]	0.0012	–	−0.0020
II[a]	–	0.0018	−0.00002
III[a]	0.0015	–	0.0150
IV[a]	–	0.0016	0.0313

All values are given in Å

[a] Variations in the bond lengths of the proton donors H–F (X = F) and H–CF₃ (X = CF₃) of the Y···H–X H-bonds with Y = O (**I** and **III**) or N (**II** and **IV**)

coworkers [53] in studies of a series of halo-hydrocarbons. In this insight, the characterization of the NH_3···HCF_3 complex based on its frequency shift is obscure whether MP2/6-311++G(d,p) is the standard level of calculation, what is not observed in H_2O···HCF_3 even though its blue-shift of $+35.4$ cm^{-1} differs from other works, e.g., the value of $+10$ cm^{-1} revised by Hobza and Havlas [54], but is quite near to $+33$ documented by Kryachko and Zeegers-Huyskens [55]. Independently, besides these findings the most important is the real elucidation of this complex on the basis of vibrational analysis.

Electronic parameter and NBO analysis

The values of the uncorrected H-bond energies ($\Delta E = E_{supermolecule} - E_{isolated\,monomers}$) and with corrections ($\Delta E^C = \Delta E + BSSE + ZPE$) are listed in Table 3. These ΔE^C values are a reflection of the interaction strength in the circumstances that the electronic charge transference amounts (ΔQ) between molecular frontier orbitals corroborate with this in full [56, 57]. Figure 2 illustrates the relationship between the values of the BSSE correction H-bond energy and intermolecular charge transfer moieties computed via NBO (ΔQ^{NBO}) and QTAIM (ΔQ^{QTAIM}) conditions, and the Eqs. (3) and (4) give support in this analysis:

$$\Delta E^C = 530.23\Delta Q^{NBO} - 8.10, \quad R^2 = 0.999 \quad (3)$$

$$\Delta E^C = 473.08\Delta Q^{QTAIM} - 5.52, \quad R^2 = 0.994 \quad (4)$$

It can be seen that the correlation between ΔE^C and ΔQ modeled by NBO is slightly better in comparison with QTAIM, which is often considered one of the most efficient approaches for measuring the charge transfer [58, 59]. Also, the complexes of HCF_3 are much less stable in

Table 2 Values of the new vibrational modes (H-bond stretch frequency) and red- and blue-shift effects (Δv^{str} and I_c^{str}/I_m^{str}) of the **I–IV** complexes obtained from the MP2/6-311++G(d,p) calculations

IR modes	H-bonded complexes			
	I	II	III	IV
$v_{Y\cdots H}^{str}$	114.0	120.1	223.2	265.7
$I_{Y\cdots H}^{str}$	0.54	0.73	5.84	7.67
v_{O-H}^{str}	3874.2	–	3881.9	–
Δv_{O-H}^{str}	−13.0	–	−5.3	–
$I_{O-H,c}^{str}$	18.4	–	135.7	–
$I_{O-H,c}^{str}/I_{O-H,m}^{str}$	1.4	–	10.3	–
v_{H-X}^{str}	3259.4	3220.7	3851.2	3480.2
Δv_{H-X}^{str}	+35.4	−3.3	−347.2	−718.3
$I_{H-X,c}^{str}$	1.19	10.7	795.2	1498.4
$I_{H-X,c}^{str}/I_{H-X,m}^{str}$	0.03	0.30	5.6	10.6
v_{N-H}^{str}	–	3515.6	–	3225.3
Δv_{N-H}^{str}	–	−10.9	–	−1.2
$I_{N-H,c}^{str}$	–	0.33	–	108.4
$I_{N-H,c}^{str}/I_{N-H,m}^{str}$	–	0.20	–	65.3

Values of v^{str} and I are given in cm^{-1} and km mol^{-1}, respectively

The Y···H–X H-bonds with Y = O (**I** and **III**) or N (**II** and **IV**)

comparison to those wherein the hydrofluoric acid is the proton donor, e.g., **III** is twice strongly bonded than **I** and, amazingly the stabilization of **IV** is the beyond of triple than anyone of **I** or **II**. However, the values of charge transfer presented above indicate a measurement of the electron fraction transferred along the proton donor molecule as a whole, i.e., the charge transfer is not concentrated in H–X, although in the case of X = CF₃(HCF_3) is mostly dispersed among the fluorine atoms, and therefore the interpretation of the frequency shifts in the proton donors can be seriously compromised [60].

In Table 3 are also listed the other parameters derived from NBO computations, such as the percentage of the s and p orbitals of X (X = F, and C not CF₃). About these ones, it should be focused the p orbitals, since its variance is a consequence of the Bent rule for chemical bonds, whose adaptation to hydrogen bond studies made by Grabowski revealed that the contribution of the s orbitals of X must be enhanced upon complexation [61]. According to the results of 1.35 (**I**), 1.74 (**II**), 4.41 (**III**), and 6.98 (**IV**), besides these values be in total concordance with the insight quoted above, a systematic and efficient relationship with the corrected H-bond energies is stated [see Eq. (5)], as can be seen in Fig. 3.

$$\Delta E^C = -4.171\Delta\%s_X - 4.142, \quad R^2 = 0.995 \quad (5)$$

By this picture, some considerations should be carefully interpreted. First of all, it can be seen that **IV** is the strongly
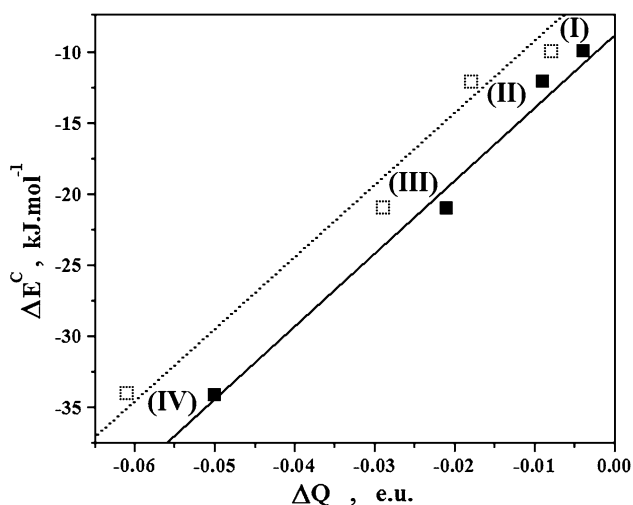
Table 3 Values of the H-bond energies (uncorrected and corrected), charge transfers (ΔQ), and NBO parameters of the **I–IV** complexes obtained through the MP2/6-311++G(d,p) calculations

Parameters	H-bonded complexes			
	I	**II**	**III**	**IV**
ΔE	−19.13	−22.32	−42.07	−55.95
ΔZPE	3.93	4.55	11.99	12.69
BSSE	5.32	5.70	9.14	9.18
ΔE^C	−9.88	−12.07	−20.94	−34.08
ΔQ^{NBO}	−0.0040	−0.0090	−0.0210	−0.0500
ΔQ^{QTAIM}	−0.0080	−0.0180	−0.0290	−0.0061
$\Delta E_{n(Y) \to \sigma*(H-X)}$	4.1	6.53	17.5	37.1
$\%sH$	99.83	99.82	99.61	99.56
$\Delta\%sH$	−0.03	−0.04	−0.09	−0.14
$\%sX$	31.57	31.96	25.73	28.30
$\Delta\%sX$	1.35	1.74	4.41	6.98
$\%pH$	0.17	0.18	0.39	0.44
$\Delta\%pH$	0.03	0.04	0.14	0.19
$\%pX$	68.22	67.84	74.16	71.60
$\Delta\%pX$	−1.36	−1.74	−4.40	−6.96

Values of ΔE, ΔZPE, BSSE, ΔE^C, and $\Delta E_{n(Y) \to \sigma*(H-X)}$ are given in kJ mol^{-1}

Values of ΔQ are given in electronic units (e.u.)

Values of $\%s$ and $\%p$ are related to the proton donor within the intermolecular model Y···H–X of the hydrogen bonds with X = CF$_3$ (**I** and **II**) or F (**III** and **IV**)

Fig. 2 Relationship between the corrected H-bond energies and charge transfer amounts of the **I–IV** complexes

Fig. 3 Relationship between the corrected H-bond energies and variation on the percentage of the s-character of X (X = CF$_3$ or F) in the **I–IV** complexes

Fig. 4 Relationship between the frequency shifts (red or blue) and variation on the percentage of the s-character of X (X = CF$_3$ or F) in the **I–IV** complexes
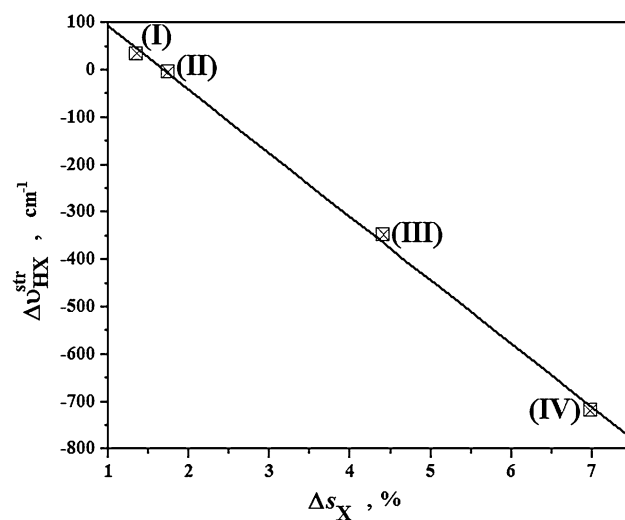
bound complex and its $\Delta\%s_X$ is the largest among the values for **I**, **II**, and **III**. Besides the H-bond energy, the intermolecular distance of **IV** is the shortest, what would lead me to assume that its frequency shift would be blue instead red because the rehybridization effect sustains this statement. Second, the increases of $\Delta\%s_X$ in **IV** as well as
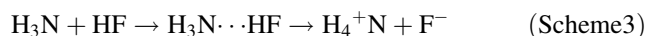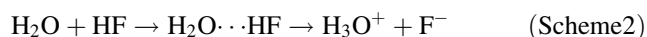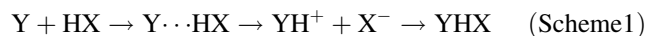
in **III** are very well correlated with the red-shift values of −347.3 and −718.3 cm^{-1} respectively, as supported by the Eq. (6) and Fig. 4:

$$\Delta\upsilon_{HX}^{str} = -134\Delta\%s_X + 226.964, \quad R^2 = 0.999 \qquad (6)$$

Third, note that only the small results of s-character are in concordance with the very slight frequency shifts of H$_2$O···HCF$_3$ and NH$_3$···HCF$_3$, and surely the blue-shift of +35.4 cm^{-1} is justified by the $\Delta\%s_X$ value of 1.35 in **I**. So, the increasing of the s-character in X sustains the weakness of the H–X bond because its p-character is reduced. At last, if an electrophilic addition reaction of H–X on Y to form

hydronium ion or ammonium cation is assumed to corroborate with these findings, often the formation of X^- due to the formation of Y–H is caused by the breaking of H–X (see Scheme 1 is the standard model while 2 and 3 make reference to **III** and **IV**) and the increasing and reduction of *s*- and *p*-characters are in line with this, and in addition the forward X^- entity means less polarizability associated with a disfiguration of the overlap molecular orbital of the proton donors [62].

$$Y + HX \rightarrow Y \cdots HX \rightarrow YH^+ + X^- \rightarrow YHX \quad (\text{Scheme1})$$

$$H_2O + HF \rightarrow H_2O \cdots HF \rightarrow H_3O^+ + F^- \quad (\text{Scheme2})$$

$$H_3N + HF \rightarrow H_3N \cdots HF \rightarrow H_4^+N + F^- \quad (\text{Scheme3})$$

In another point of view, the NBO energy computed through the Eq. (1) also reinforce the current thesis that stronger bound complexes (**III** and **IV**) with largest red-shift effects are formed with drastic enhancements on *s*-character of X (F or CF_3). This insight is validated by the Eq. (7) [63] optimized in agreement with the Fig. 5, in which can be perceived that stronger hydrogen-bonded complexes really present the largest *s*-character variation in X.

$$\Delta E_{n(Y) \rightarrow \sigma*(H-X)} = 5.674\Delta\%s_X - 4.233, \quad R^2 = 0.988 \quad (7)$$

QTAIM analysis and prediction of the interaction strength

In Table 4 are listed the values of the topological parameters: ρ, $\nabla^2\rho$, G, and U. Moreover, the results of the
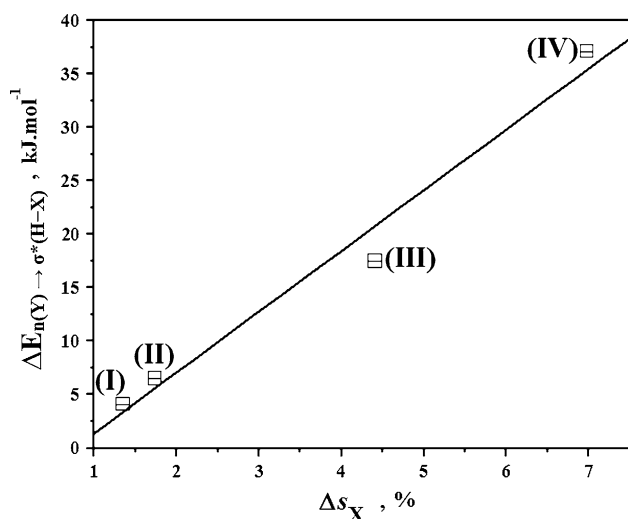

Fig. 5 Relationship between the NBO binding energies and variation on the percentage of the *s*-character of X (X = CF_3 or F) in the **I–IV** complexes

QTAIM atomic radii calculated by taking into account the BCP of H–X is also available. According to the Eq. (2), the positive results for $\nabla^2\rho$ show that **I–IV** complexes are intermolecularly stabilized. In terms of charge density, the low values of ρ also corroborates to that [64, 65]. However, it should be highlighted that albeit **IV** is strongly bound its intermolecular charge density is relatively high not only in comparison with **I–III**, but also with other H-bonded systems [66–68]. Concordant with the literature [69–71], the absolute linear coefficient (R^2) of 0.986 [Eq. (8)] yielded by the Fig. 6 indicates a good relationship between the results of ΔE^C and $\rho_{Y\cdots HX}$:

$$\Delta E^C = -673.155\rho_{Y\cdots HX} - 0.505, \quad R^2 = 0.986 \quad (8)$$

Meanwhile, one much more efficient procedure to predict the interaction strength can be performed through the association between molecular parameters and topological descriptors of the proton donors (Δmol), such as ρ_{HX} and $\nabla^2\rho_{HX}$. Although it has been used specific referential points on the intermolecular structure (Δr_{HX}), instead of these here and in agreement with other works the frequency shifts ($\Delta\upsilon_{HX}^{str} = \upsilon_{HX,complex}^{str} - \upsilon_{HX,monomer}^{str}$) were used in Eq. (9) because best correlations are obtained.

Table 4 Values of the intermolecular topological parameters of the **I–IV** complexes determined by QTAIM integrations

Parameters	H-bonded complexes			
	I	**II**	**III**	**IV**
$\rho_{Y\cdots H}$	0.01405	0.01549	0.03402	0.04778
$\nabla^2\rho_{Y\cdots H}$	0.05612	0.05015	0.14960	0.13172
$G_{Y\cdots H}$	0.01177	0.01070	0.03550	0.04027
$U_{Y\cdots H}$	−0.00951	−0.00886	−0.03370	−0.04761
$-G_{Y\cdots H}/U_{Y\cdots H}$	1.23764	1.20767	1.05341	0.84583
$H_{Y\cdots H}$	0.00226	0.00184	0.00180	−0.00734
ρ_{H-X}	0.31882	0.31788	0.34639	0.32361
$\nabla^2\rho_{H-X}$	−1.32660	−1.32786	−2.9130	−2.59621
G_{H-X}	0.01706	0.01666	0.07279	0.07663
U_{H-X}	−0.36577	−0.36529	−0.87375	−0.80232
$-G_{H-X}/U_{H-X}$	0.04664	0.04560	0.08333	0.09551
H_{H-X}	−0.34871	−0.34863	−0.80009	−0.72569
r_H	0.3433	0.3393	0.1364	0.1384
Δr_H	−0.0149	−0.0188	−0.0044	−0.0024
r_X	0.7421	0.7481	0.7952	0.8094
Δr_X	0.0128	0.0188	0.0194	0.0338

Values of ρ and $\nabla^2\rho$ are given in e.a$_o^{-3}$ and e.a$_o^{-5}$, respectively

Values of G, U, and H are given in electronic units (e.u.)

Values of r_H, Δr_H, r_X, and Δr_X are given in Å

The Y···H–X H-bonds with Y = O (**I** and **III**) or N (**II** and **IV**) and X = CF_3 (**I** and **II**) or F (**III** and **IV**)
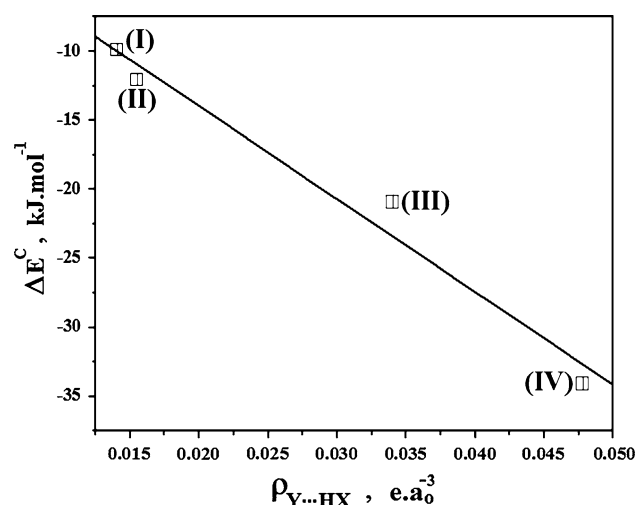
Fig. 6 Relationship between the corrected H-bond energies and intermolecular electronic densities of the **I–IV** complexes

$$\Delta mol = [(|\Delta\upsilon_{HX}^{Str}|/\upsilon_{oHX})^2 + (|\Delta\rho_{HX}|/\rho_{oHX})^2 \\ + (|\Delta\nabla^2\rho_{HX}|/\nabla^2\rho_{oHX})^2]^{1/2} \quad (9)$$

where $\Delta\rho_{HX} = \rho_{HX,complex} - \rho_{HX,monomer}$ and $\Delta\nabla^2\rho_{HX} = \nabla^2\rho_{HX,complex} - \nabla^2\rho_{HX,monomer}$. Figure 7 and Eq. (10) show the excellent relationship between ΔE^C and Δmol.

$$\Delta E^C = -104.286\Delta mol - 6.842, \quad R^2 = 0.992 \quad (10)$$

These H-bond energy values keep indicating that **IV** is the strongest bound system, not only because its intermolecular distance is shorter than 1.80 Å, but mainly because the relationship $-G_{N\cdots H}/U_{N\cdots H}$ of 0.84583 is smaller than 1 as well as the total electronic density energy (H) is negative, whose value is -0.00734 e.u., i.e.,

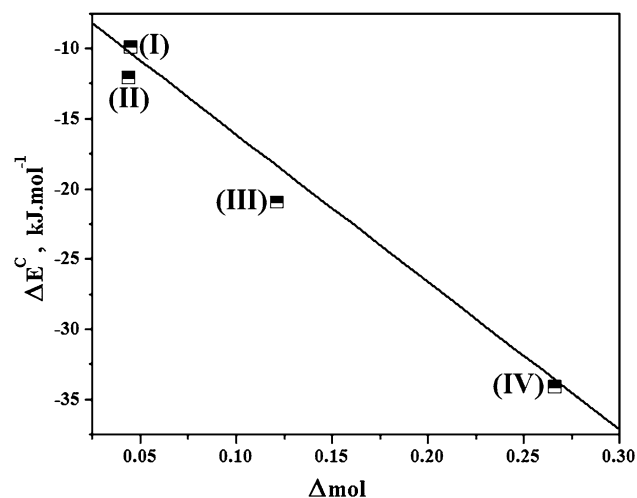**Fig. 7** Relationship between the corrected H-bond energies and molecular parameters (vibration associated with topology) of the **I–IV** complexes
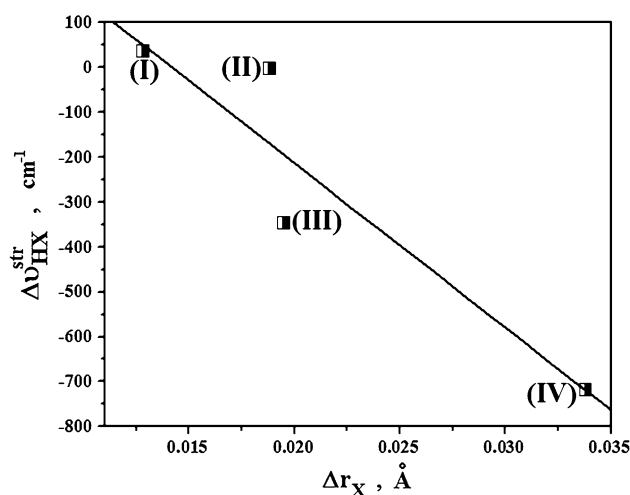

Fig. 8 Relationship between the frequency shifts (red or blue) and variation on the percentage of the *s*-character of X (X = CF$_3$ or F) in the **I–IV** complexes

the NH$_3\cdots$HF complex is partially covalent bound. Regarding the other systems, the values of $-G/U$ and H are 1.23764 and 0.00226 e.u. for **I**, 1.20767 and 0.00184 e.u. for **II**, and finally 1.05341 and 0.00180 e.u. for **III**, respectively. Even the intermolecular distance of **III** is smaller than 1.80 Å, precisely the computed value is 1.7310 Å, H$_2$O$\cdots$HF is almost partially covalent.

Recently, a QTAIM study for hydrogen bond interactions revealed that the variation on bond radii computed in the BCP between H and X within H–X bond path can explain the frequency shift of this oscillator as follows: $\Delta r_X > \Delta r_H$ if red-shift occur or $\Delta r_X < \Delta r_H$ for blue-shift. Indeed, the frequency shifts of **II–IV** agree with this rule, what is not observed in **I** because the respective values for Δr_C of 0.0128 and Δr_H of -0.0149 Å not justify the blue-shift of $+35.4$ cm^{-1}. Thus, the relationship between the frequency shifts $(\Delta\upsilon_{HX}^{str})$ of the proton donors and the variations on the BCP radii of X (Δr_X) along the H–X axis is plotted in Fig. 8, in which a satisfactory linear correlation coefficient (R^2) of 0.928 is obtained through the Eq. (11):

$$\Delta\upsilon_{HX}^{str} = -36671.106\Delta r_X + 520.244, \quad R^2 = 0.928 \quad (11)$$

Conclusions and highlights

In summary, the theoretical study presented in this current work raises an important question related to the hydrogen bond strength, mainly those possessing covalent character. The intermolecular model complexes of H$_2$O$\cdots$HCF$_3$, NH$_3\cdots$HCF$_3$, H$_2$O$\cdots$HF, and NH$_3\cdots$HF have shown systematic tendencies, either in structural or vibrational analysis. Regarding the H-bond energies, the computed values

are in good correlation with the intermolecular charge transfers, as well as with the intermolecular density amounts determined topologically by the QTAIM protocol. Furthermore, the most incisive conclusion found in this work is that the interpretation of the frequency shifts at light of the BCP radii of X is fails, in special for the weakest bound complex of $H_2O \cdots HCF_3$ in which its blue-shift of $+35.4$ cm^{-1} would be justified by $\Delta r_X < \Delta r_H$, what does not occur. In line with this, it is widely known that the stretch frequencies of the proton donors in weakly bound complexes often are shifted to blue-region and vice versa in regards to the strongly bound ones in which the red-shifts are manifested [18, 72]. Not only this, but the argument of the Bent rule [73] is concordant with the increase of the s-character of X (F or C), but in total disagreement with the red-shifted of the stretch frequencies of H–F and H–C once blue-shift was the expected vibrational effect. Although this new interpretation differs from chemical literature, the variation in s-character of X is well adjusted with the intermolecular strength or H-bond energies, frequency shifts either from red or blue nature, and NBO binding energies.

References

1. Goymer P (2012) Nat Chem 4:863–864
2. Filho EBA, Ventura E, do Monte SA, Oliveira BG, Junior CGL, Rocha GB, Vasconcellos MLAA (2007) Chem Phys Lett 449:336–340
3. Molčanov K, Portada T, Čaplar V, Jokić M, Makarević J, Vujičić NS, Štefanić Z, Žinić M, Kojić-Prodic B (2013) Struct Chem 24:597–609
4. Fumino K, Peppel T, Geppert-Rybczyńska M, Zaitsau DH, Lehmann JK, Verevkin SP, Köckerling M, Ludwig R (2011) Phys Chem Chem Phys 13:14064–14075
5. Elsaesser T (2009) Acc Chem Res 42:1220–1228
6. Shen J, Wang H, Xia Y (2013) Struct Chem 24:559–571
7. Desiraju GR (2011) Angew Chem Int Ed 50:52–59
8. Grabowski SJ (2001) Chem Phys Lett 338:361–366
9. Oliveira BG, Ferreira FS, Araújo RCMU, Ramos MN (2007) Chem Phys Lett 427:181–184
10. Oliveira BG, Araújo RCMU, Carvalho AB, Ramos MN (2007) Chem Phys Lett 43:390–393
11. Gu Q, Trindle C, Knee JL (2012) J Chem Phys 137: 091101–091104
12. Grabowski SJ (2011) Chem Rev 111:2597–2625
13. Isaacs ED, Shukla A, Platzman PM, Hamann DR, Barbiellini B, Tulk CA (1999) Phys Rev Lett 82:600–603
14. Martin TW, Derewenda ZS (1999) Nat Struct Biol 6:403–406
15. Oliveira BG (2012) Comput Theor Chem 998:173–182
16. Oliveira BG, Vasconcellos MLAA, Olinda RR, Filho EBA (2009) Struct Chem 20:81–90
17. Oliveira BG, Araújo RCMU, Pereira FS, Lima EF, Silva WLV, Carvalho AB, Ramos MN (2008) Quim Nova 31:1673–1679
18. Oliveira BG, Araújo RCMU, Ramos MN (2009) J Mol Struct (THEOCHEM) 908:79–83
19. Oliveira BG, Araújo RCMU, Carvalho AB, Ramos MN (2009) Struct Chem 20:663–670
20. Oliveira BG, Araújo RCMU, Carvalho AB, Ramos MN (2007) Quim Nova 30:1167–1170
21. Oliveira BG, Araújo RCMU, Carvalho AB, Ramos MN, Hernandes MZ, Cavalcante KR (2007) J Mol Struct (THEOCHEM) 802:91–97
22. Oliveira BG, Leite LFCC (2009) J Mol Struct (THEOCHEM) 915:38–42
23. Oliveira BG, Vasconcellos MLAA (2009) Inorg Chem Commun 12:1142–1144
24. Oliveira BG (2013) Phys Chem Chem Phys 15:37–79
25. Umeyama H, Morokuma K (1977) J Am Chem Soc 99:1316–1332
26. Buckingham AD, Fowler PW, Hutson JM (1988) Chem Rev 88:963–988
27. Oliveira BG, Lima MCA, Pitta IR, Galdino SL, Hernandes MZ (2010) J Mol Model 16:119–127
28. Davidson ER, Jarzecki AA, Hirao K (1999) Recent advances in multireference methods, World Scientific
29. Graham D, Fletcher GD, Fedorov DG, Pruitt SR, Windus TL, Gordon MS (2012) J Chem Theory Comput 8:75–79
30. da Silva JBP, Neto BB, Ramos MN, Bruns RE (1998) Chemom Intell Lab Syst 44:187–195
31. van Duijneveldt FB, Duijneveldt-van de Rijdt JGCM, van Lenthe JH (1994) Chem Rev 94:1873–1885
32. Nesbitt DJ (1988) Chem Rev 88:843–870
33. Oliveira BG, Araújo RCMU, Ramos MN (2009) J Mol Struct (THEOCHEM) 944:168–172
34. Weinhold F, Landis CR (2001) Chem Educ Res Pract Eur 2:91–104
35. Reed AE, Curtiss LA, Weinhold F (1988) Chem Rev 88:899–926
36. Popelier PLA, Bader RFW (1992) Chem Phys Lett 189:542–548
37. Popelier PLA (1995) J Phys Chem 99:9747–9754
38. Bader RFW (1990) Atoms in molecules: a quantum theory. Oxford University Press, Oxford
39. Bader RFW (1991) Chem Rev 91:893–928
40. Brindle CA, Chaban GM, Gerber RB, Janda KC (1005) Phys Chem Chem Phys 7:945–954
41. Bulychev VP, Grigoriev IM, Gromovaa EI, Tokhadze KG (2005) Phys Chem Chem Phys 7:2266–2278
42. Sadlej AJ, Bludský O, Špirko V (1993) Coll Czech Chem Commun 58:2813–2830
43. Fraser GT, Lovas FJ, Suenram RD, Nelson DD, Klemperer W (1986) J Chem Phys 84:5983–5988
44. Gaussian 03, Revision B.04, Frisch MJ, Trucks GW, Schlegel HB, Scuseria GE, Robb MA, Cheeseman JR, Montgomery Jr JA, Vreven T, Kudin KN, Burant JC, Millam JM, Iyengar SS, Tomasi J, Barone V, Mennucci B, Cossi M, Scalmani G, Rega N, Petersson GA, Nakatsuji H, Hada M, Ehara M, Toyota K, Fukuda R, Hasegawa J, Ishida M, Nakajima T, Honda Y, Kitao O, Nakai H, Klene M, Li X, Knox JE, Hratchian HP, Cross JB, Adamo C, Jaramillo J, Gomperts R, Stratmann RE, Yazyev O, Austin AJ, Cammi R, Pomelli C, Ochterski JW, Ayala PY, Morokuma K, Voth GA, Salvador P, Dannenberg JJ, Zakrzewski VG, Dapprich S, Daniels AD, Strain MC, Farkas O, Malick DK, Rabuck AD, Raghavachari K, Foresman JB, Ortiz JV, Cui Q, Baboul AG, Clifford S, Cioslowski J, Stefanov BB, Liu G, Liashenko A, Piskorz P, Komaromi I, Martin RL, Fox DJ, Keith T, Al-Laham MA, Peng CY, Nanayakkara A, Challacombe M, Gill PMW, Johnson B, Chen W, Wong MW, Gonzalez C, Pople JA, Gaussian, Inc., Pittsburgh PA, 2003
45. Keith TA (2011) AIMAll Version 11.05.16
46. Rowland RS, Taylor R (1996) J Phys Chem 100:7384–7391

47. Bondi A (1964) J Phys Chem 68:441–451
48. Klein RA (2002) J Am Chem Soc 124:13931–13937
49. Araújo RCMU, da Silva JBP, Ramos MN (1995) Spectrochim Acta A 51:821–830
50. Araújo RCMU, Ramos MN (1996) J Mol Struct (THEOCHEM) 366:233–240
51. Rozas I, ALkorta I, Elguero J (1997) J Phys Chem A 101:9457–9463
52. Botschwina P, Oswald R (2005) Z Phys Chem 219:399–420
53. Delanoye SN, Herrebout WA, van der Veken B (2002) J Am Chem Soc 124:11854–11855
54. Hobza P, Havlas Z (2000) Chem Rev 100:4253–4264
55. Kryachko ES, Zeegers-Huyskens T (2001) J Phys Chem A 105:7118–7125
56. Oliveira BG, Araújo RCMU (2007) Quim Nova 30:791–796
57. Oliveira BG, Araújo RCMU (2012) Can J Chem 90:368–375
58. Oliveira BG, Araújo RCMU, Ramos MN (2008) Struct Chem 19:185–189
59. Oliveira BG, Ramos MN (2010) Int J Quantum Chem 110:307–316
60. Oliveira BG, Araújo RCMU (2012) J Mol Model 18:2845–2854
61. Grabowski SJ (2011) J Phys Chem A 115:12789–12799
62. Oliveira BG, Araújo RCMU, Carvalho AB, Lima EF, Silva WLV, Ramos MN, Tavares AM (2006) J Mol Struct (THEOCHEM) 775:39–45
63. Kolandaivel P, Nirmala V (2004) J Mol Struct 694:33–38
64. Oliveira BG, Araújo RCMU, Ramos MN (2008) Struct Chem 19:665–670
65. Oliveira BG, Araújo RCMU, Silva JJ, Ramos MN (2010) Struct Chem 21:221–228
66. Parthasarathi R, Raman SS, Subramanian V, Ramasami T (2007) J Phys Chem A 111:7141–7148
67. Huang Z, Yu L, Dai Y (2010) Struct Chem 21:565–572
68. Mo Y (2012) J Phys Chem A 116:5240–5246
69. Grabowski SJ (2000) J Mol Struct 553:151–156
70. Wojtulewski S, Grabowski SJ (2002) J Mol Struct 605:235–240
71. Grabowski SJ, Sokalski WA, Leszczynski J (2004) J Phys Chem A 108:5823–5830
72. Murray JS, Concha MC, Lane P, Hobza P, Politzer P (2008) J Mol Model 14:699–704
73. Bent HA (1961) Chem Rev 61:275–311